

Open Research Online

The Open University's repository of research publications and other research outputs

Charge-coupled devices for the ESA Euclid M-class mission

Conference or Workshop Item

How to cite:

Endicott, J.; Darby, S.; Bowring, S.; Eaton, T.; Grey, A.; Swindells, I.; Wheeler, R.; Duvet, L.; Cropper, M.; Walton, D.; Holland, A.; Murray, N. and Gow, J. (2012). Charge-coupled devices for the ESA Euclid M-class mission. In: High Energy, Optical, and Infrared Detectors for Astronomy V, 1-6 Jul 2012, Amsterdam.

For guidance on citations see [FAQs](#).

© 2012 Society of Photo-Optical Instrumentation Engineers

Version: Accepted Manuscript

Link(s) to article on publisher's website:

<http://dx.doi.org/doi:10.1117/12.926323>

<http://proceedings.spiedigitallibrary.org/proceeding.aspx?articleid=1363302>

Copyright and Moral Rights for the articles on this site are retained by the individual authors and/or other copyright owners. For more information on Open Research Online's data [policy](#) on reuse of materials please consult the policies page.

oro.open.ac.uk

Charge-Coupled Devices for the ESA Euclid M-class Mission

J. Endicott^{*a}, S. Darby^a, S. Bowring^a, D. Burt^a, T. Eaton^a, A. Grey^a, I. Swindells^a, R. Wheeler^a,
L. Duvet^b, M. Cropper^c, D. Walton^c, A. Holland^d, N. Murray^d & J. Gow^d

^ae2v technologies (UK) Ltd, 106 Waterhouse Lane, Chelmsford, CM1 2QU, UK

^bEuropean Space Agency, Keplerlaan 1, 2200AG Noordwijk, The Netherlands

^cMullard Space Science Laboratory, Holmbury St. Mary, Dorking, Surrey RH5 6NT, UK

^de2v Centre for Electronic Imaging, DPS, The Open University, Milton Keynes, MK7 6AA, UK

ABSTRACT

The European Space Agency has funded e2v's development of an image sensor for the visible instrument in the Euclid space telescope. Euclid has been selected for a medium class mission launch opportunity in 2020. The project aims to map the dark universe with two complementary methods; a galaxy red-shift survey and weak gravitational lensing using near infrared and visible instruments. The baseline for the visible instrument was to be the CCD203-82, which has been successfully flown on NASA's Solar Dynamics Observatory. However, to optimise the device for Euclid, e2v have designed and manufactured the CCD273-84. This device has a higher-responsivity lower-noise amplifier, enhanced red response, parallel charge injection structures and narrower registers which improve low signal charge transfer efficiency. Development models for Euclid have been manufactured with a thinner gate dielectric than standard for improved tolerance to ionising radiation. This paper describes the imager sensor in detail and focuses on the novel aspects of the device, package and interface.

Keywords: Si CCDs, advancements in detector design and fabrication, novel detector designs

1. INTRODUCTION

Euclid has been selected for launch in 2020 to map the dark universe. The data generated by the telescope will be used to study the role of dark matter and energy in the evolution of the Universe. It will enable current models to be tested including the validity of modifications to general relativity. The dataset will also be utilised in wider studies beyond the scope of the mission for many years to come¹.

The visible instrument will be dedicated to the weak gravitational lensing method where the mission will survey 15,000 square degrees of the extragalactic sky with a resolution of 0.2 arcsecond in the wavelength range of 550-900nm. The survey will measure the shapes of more than 2 billion galaxies to study the orientation and distortion of these by the gravitational field along the optical path. The results of the survey will reveal the dark matter distribution and cosmological structures from their gravitational effect on the images.

The precision with which the Euclid visible image sensors can measure the shapes of galaxies is of paramount importance to the success of the mission. In order to achieve this aim, e2v Charge-Coupled Devices (CCDs) are selected over CMOS image sensors or infrared detectors operated in the visible range because of their higher dynamic range, lower noise, superior uniformity and extensive heritage in space missions.

The baseline sensor for the mission was e2v's CCD203-82, initially developed for NASA's Solar Dynamics Observatory (SDO) Atmospheric Imaging Assembly (AIA) and Helioseismic and Magnetic Imager (HMI) instruments. With the launch of SDO in 11th of February 2010, 6 sensors are currently in operation on the AIA and HMI instruments.

The CCD203-82 is a 4k x 4k pixel sensor with each pixel 12 μm x 12 μm . To optimise the device for Euclid, e2v have designed and manufactured the CCD273-84. This device has a higher-responsivity lower-noise amplifier, enhanced red response through the adoption of thicker deep depleted silicon, parallel charge injection structures and narrower registers which improve low signal charge transfer efficiency with respect to the CCD203-82.

This paper describes the CCD273-84 sensor in detail and focuses on the novel aspects of the device, package and interface.

2. CHANGES TO THE CCD203-82

The CCD203-82 was designed to accommodate binning of multiple lines into the serial read-out register. This feature has two impacts on the performance of the sensor. The first is that the CCD output amplifier has to have a lower responsivity and correspondingly higher noise than a circuit that is optimised for the capacity of the image pixel. The second is that the serial register width needs to be increased to handle the large binned signals.

The Euclid visible instrument requires the full resolution afforded by the image area and will not need to use the binning capability. A higher-responsivity lower-noise amplifier can thus be used. This change also led to the removal of the second output gate from the CCD203-82 as the design was revised to make the CCD273-84.

With a higher responsivity amplifier the charge handling capacity of the serial register now far exceeds the requirements of the image area pixel. A narrower serial register can thus be used as this confines the charge to a smaller volume of silicon and improves the charge transfer efficiency, particularly later in the mission when the effects of displacement damage from energetic particles begin to take their toll. This change helps preserve the signals representing the shapes of the galaxies during the serial transfer of the charge packets during read-out.

A third change to the CCD203-82 was identified for the Euclid CCD development. The instrument will use 4 output ports to read out each 2k x 2k quadrant. In this scheme the device is read out without transferring charge across the centre of the detector. A charge injection structure can thus be included in the centre of the device to inject a line of charge that can be transferred through the device in over-scan rows when the images are read out. The injected charge can fill any empty traps in the device and could potentially improve the charge transfer efficiency. The incorporation of the charge injection structure will sacrifice 4 rows of the image area, representing less than 0.1% of each device. If the improvement is considered to be less important than the loss of image area, the structure can be replaced by imaging pixels for the flight devices.

The three improvements to the baseline CCD have been included in the design of a breadboard model for Euclid. Charge injection schemes will be studied in detail using the baseline operating conditions for the Euclid CCDs. It is envisaged that each image will be acquired with an integration time of at least 400 seconds at a temperature of -120°C. The low temperature is specified to minimise dark current to such a level that the long exposure time enables faint sources to be detected.

Although there can be some advantage in optimising the read-out rates and temperature, the charge transfer efficiency is fundamentally limited by the different trap species generally present in silicon. However, these detectors will see a diffuse optical background that may serve to keep the traps filled. The combination of the diffuse optical background and charge injection described earlier may prove to limit the effects of radiation damage and extend the performance and potential duration of the mission.

3. EUCLID CCD273 DESIGN DETAILS

Figure 1 shows a schematic of the CCD273-84. The device is split into top and bottom halves by a central Charge Injection (CI) structure. The CI structure consists of a central drain with adjacent pairs of injection gates. The second gate, IG2, contains a “notch” to allow a small controlled amount of charge to be transferred into the image pixels. The CI structure is discussed in detail in below.

Between the central CI structure and the registers at the top and bottom of the device are the two image area sections, A and D. The nomenclature arises from e2v designs of large area devices which have the flexibility to be manufactured as split frame transfer devices, and thus require image sections A, B, C and D.

Each image section is 2066 rows by 4096 columns where each pixel is 12 x 12 μm^2 with a four phase electrode structure. Between the images areas and the registers is a transfer gate that enables the critical transfer into the register to be independently controlled.

The images are read out through 4 ports, one at each end of the split registers at the top and bottom of the device. A full half image section can be read out through a single amplifier by reversing the direction of charge transfer in the second

half of the register. The registers consist of three phase elements, which is the standard approach for the majority of e2v's devices. The register channel width allows a linear signal handling capability of up to 150% of that of the pixel Full Well Capacity (FWC).

Each output port consists of a pair of read out amplifier circuits. The “real” circuit is used to read out the signal from the CCD, and the “dummy” circuit can be used to suppress common mode noise. Inputting these channels to an off-chip differential amplifier suppresses correlated noise but increases uncorrelated noise by $\sqrt{2}$. Should the dummy amplifiers not be required, they can be powered down through a separate Output Drain supply.

The output circuit of the device was a duplication of a standard low-noise high-responsivity amplifier design. Minor modification were made to widen the reset transistor and the channel across the output gate to alleviate the narrow channel effect which is more severe on deep depleted material. The narrow channel is known to cause a higher threshold voltage in transistors.

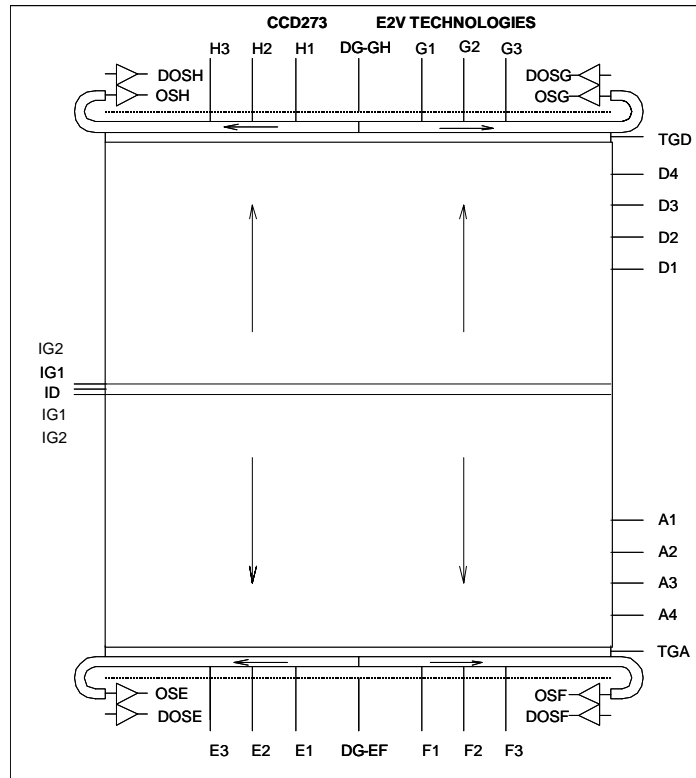


Figure 1 is a schematic of the CCD273-84.

The novel aspects of the CCD273-84 design were the use of a thinner gate dielectric in conjunction with high resistivity (1500 ohm.cm) deep depleted material and the introduction of the charge injection structure.

The use of thinner gate dielectrics and deep depleted material has been demonstrated on previous devices independently. For example, the thinner gate dielectric was used on the CCD203-82s flown on NASA's Solar Dynamics Observatory in 2010 and the Gaia Red Photometer CCDs were manufactured on deep depleted material. The predicted performance for the Euclid CCD273 was determined from rigorous device modeling, supported by compensated comparisons with existing measurements.

The charge injection structure incorporated in the Euclid CCD design represents an improvement on previous realisations of the function. In the past, charge injection has been implemented using a single gate, or pair of gates across the top of a device. Figure 2 shows some data generated by operating a previous device with continuous row-by-row parallel clocking. Charge was injected for 100 rows before switching off the charge injection for 100 rows. This was repeated four times, so that an image with a 1,000 rows was produced. The profile along a column shows the transition in the image between rows where charge is and is not injected is very sharply defined, indicating reliable switching and

low charge transfer inefficiency. The profile along a row shows short range column-to-column non-uniformity in the injected signal. From the results shown in Figure 2 the short range variation is equivalent to a random voltage difference of about 200 mV peak-peak, probably through threshold effects. The long range variation is of a similar value, probably through the modulating influence of clocking the adjacent image phases.

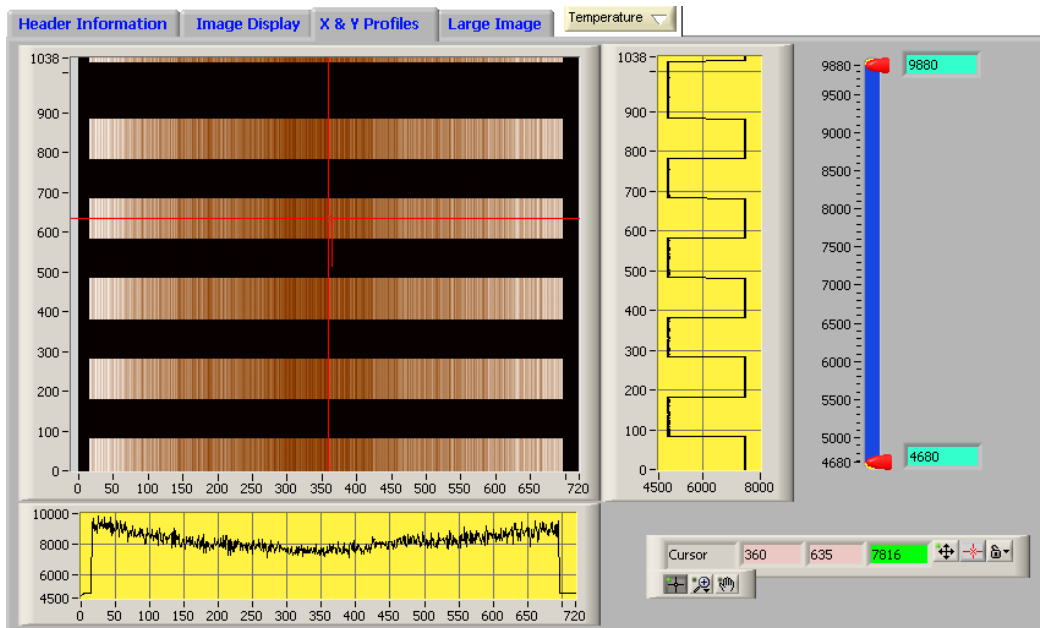


Figure 2 shows an image of a sequence of charge injection over several groups of 100 rows. The profile to the right is taken along the central column and the profile to the bottom of the image is taken along a row in the 4th block of injected signal from the bottom. The values are signal in ADU.

For Euclid where the aim was to inject uniform low levels of signal to fill traps generated by radiation damage, e2v proposed and designed a “notch” within the IG2 injection gate as shown in Figure 3. The drawn notch area is 3.5 μ m long by 4 μ m wide, and is defined by a separate p-type implant which is also used to reinforce the column isolation. One proposed method of operation is shown in Figure 3 where a fixed quantity of charge can be injected into the notch by pulsing the injection drain low. Once the drain has returned to a high value, the first image phase is taken high allowing the charge to transfer from the notch into the first row.

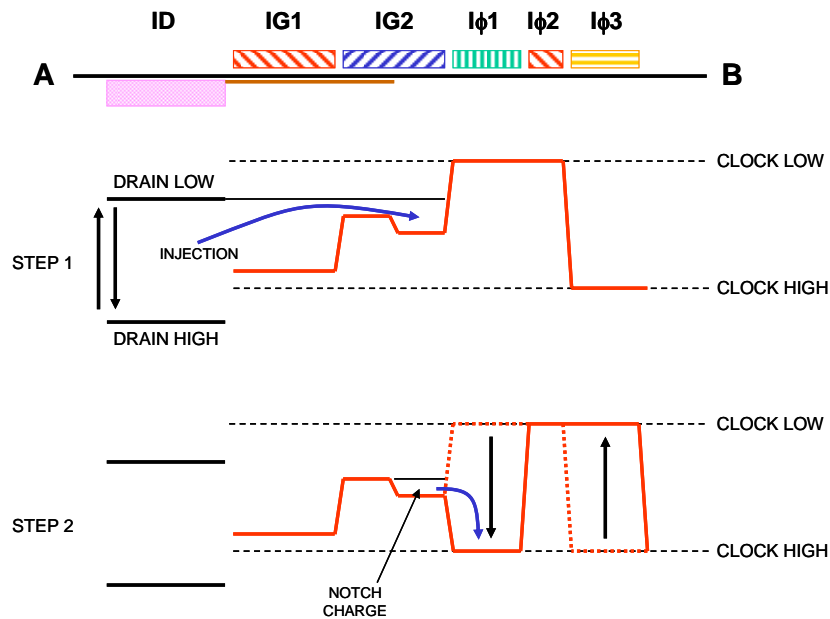


Figure 3 shows a sketch of one way to operate the Euclid CCD273 charge injection structure. The notch feature in IG2 was incorporated to provide uniform small signal injection.

The quantities of injected charge are dependent on the notch geometry and manufacturing process. For this device an injection charge of $5600e^- \pm 50\%$ was anticipated. The large uncertainty was due to the specified process combinations ($1500\Omega\text{cm}$ starting material and a thin gate dielectric) for Euclid having not been characterised for charge injection.

Figure 4 shows two row profiles for a front illuminated CCD273-84. The profiles are from single rows of injected charge into the A and D image sections of the device. The profiles show a variation of approximately $2ke^-$ across each row and a difference of $4ke^-$ in the amount of signal injected into each half. The variation along a row amounts to approximately 16mV (using a responsivity of $8\mu\text{V}/e^-$), which is a significant improvement over a simple two gate structure. The asymmetry between the injection into the top and bottom half of the device is still a subject of investigation.

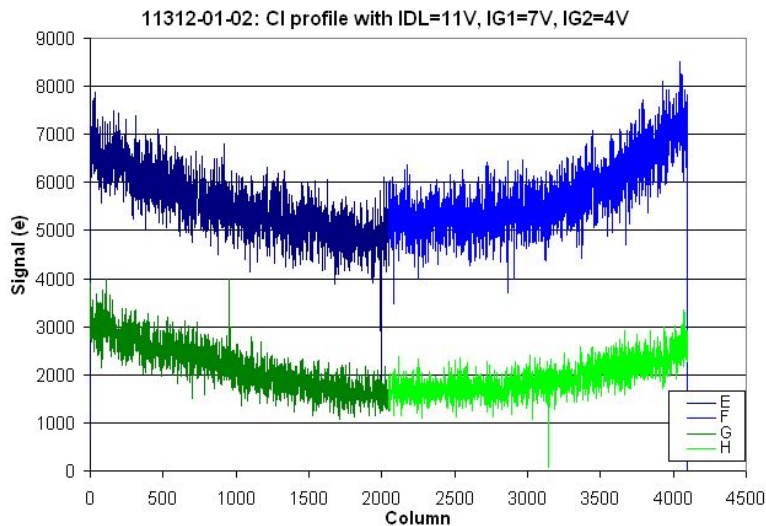


Figure 4 shows two row profiles of injected signal for a front illuminated CCD273-84.

Alternative methods of charge injection that are expected to yield further improvements in uniformity are the use of a diode cut-off method or the use of a serial parallel structure. The diode cut-off method uses a single injection gate and

constant current source. The rationale for this method is that the constant current source will uniformly fill a potential well. The downside of this approach is that it is anticipated to be harder to implement with space electronics. The serial parallel structure relies on a single small area injection gate to provide a reproducible injection level into a register. Once the register is filled, a uniform row is transferred into the image section. The downside of this technique is that each line of injected charge takes far longer to generate. Both these methods would require demonstration in a working device and currently uniform low signal level charge injection is no longer a requirement for Euclid.

The charge injection structure does have a further advantage in that the drain prevents bright sources in the lower half of the device from corrupting the corresponding column in the top half of the device. For this reason alone, the structure will be retained in the mission Flight Model requirements.

4. EUCLID PACKAGE DESIGN

The Euclid visible instrument focal plane will consist of an array 6 x 6 CCDs maintained at a temperature of -120°C. Each device is cooled by direct contact with the cold optical bench. The flexible cable between the CCD and the warm front end electronics provides a thermal break and the electrical interface. Figure 5 shows a front illuminated CCD273-84 on a handling jig with two flexible cables extending away from the package.

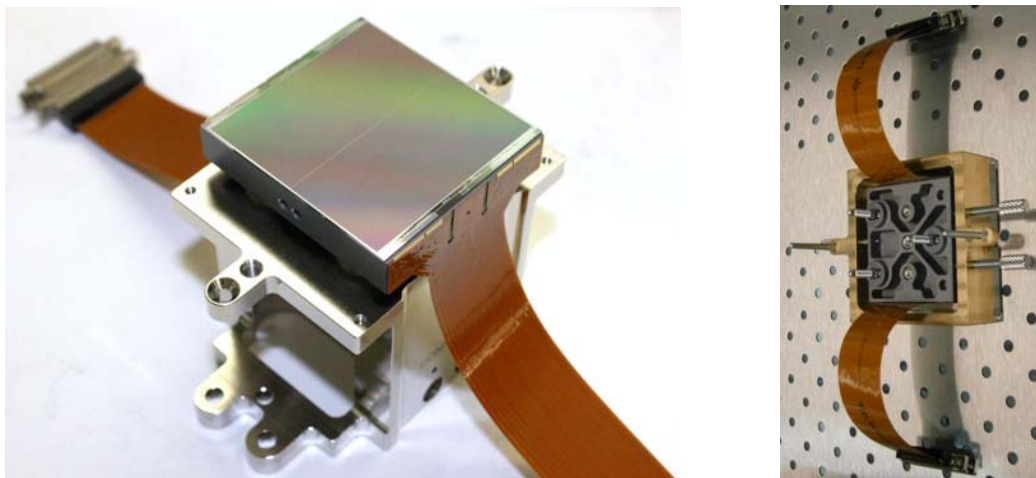


Figure 5. Figure 5 (left) shows a front illuminated CCD273-84 on a handling jig with two flexible cables extending away from the package. The picture on the right shows the reverse side of the package where the undercut holes house inserts for handling and alignment tools and the mounting studs.

The Euclid CCD package is manufactured from Silicon Carbide (SiC) and contains various undercut holes to fit threaded inserts that provide the different mechanical interfaces. Silicon carbide is a desirable material for CCD packages as it has a close thermal expansion match to silicon and a high thermal conductivity.

Figure 5 shows top surface (sky facing) and bottom surface (optical bench facing) views of the whole device assembly. The assembly consists of the die, flexible cables with micro-D connectors, Platinum Resistance Thermistors (PRTs), threaded inserts for handling rods and alignment tools, and three studs with shims attached to inserts in the package.

The studs and shims provide the mechanical and thermal interface to the instrument. The shims are clamped to undercut holes in the SiC package by the stud, and are the thermal interface for cooling the package. The studs enable the packages to be secured to the optical bench, and the combination of the studs and shims enable e2v to specify a precise package height tolerance and image area flatness.

5. KEY SPECIFICATIONS OF THE EUCLID CCD

The following table outlines the key performance parameters of the Euclid CCD at the specified characterisation temperature. The information is extracted from the Euclid CCD Specification².

Table 1 outlines the key performance parameters of the Euclid CCD.

Parameter	Specification	Target
CCD characterisation temperature, °C	-123 + 15°C	-
Pixel Size, $\mu\text{m} \times \mu\text{m}$	12.0	-
Number of Pixels, Full Frame	4096 x 4096	-
Image Area Peak-to-Valley Flatness, μm	≤ 20	-
Package Height Tolerance, μm	$\leq \pm 15$	-
Minimum Quantum Efficiency, %		
550 nm	83	86
750 nm	83	86
950 nm	23	28
Full Well Capacity, ke-	≥ 175	200
Dark Signal, e-/pixel/hr at 153K	≤ 2	0.01
Photo Response Non-Uniformity, %		
550 nm	≤ 3.0	-
750 nm	≤ 3.0	-
950 nm	≤ 5.0	-
Noise at 70kpixels/s, e- rms	≤ 3.6	2.8
Charge Transfer Efficiency		
Parallel	≥ 99.9995	-
Serial	≥ 99.9995	-
Output Amplifier Responsivity, $\mu\text{V}/\text{e-}$	6.0 – 8.0	7.0
Linearity, %	< 4.0	3.0
Power Dissipation, mW		
Static (On chip) for 4 single ports	< 52	40
Dynamic and Static (On chip) for 4 single ports	< 60	46
Mass, g	< 80	-

6. CONCLUSIONS

This paper has described the changes to the CCD203-82 that have been made to optimize a 4k x 4k CCD for the Euclid mission. The Euclid CCD273-84 device and package design details have been outlined. Specific emphasis has been given to the description of the charge injection structure as this was a novel feature of the device. Finally, an outline of the key device performance specifications has been summarised.

REFERENCES

- [1] Cropper, M. et al., “VIS: the visible imager for *Euclid*”, these proceedings, (2012).
- [2] Euclid CCD Specifications, SRE-PA/2010.051, Issue 0, Revision 1, 10/06/2010.